

ARTICLE TYPE

SimLivA – Modelling ischemia reperfusion injury in the liver: A first step towards a clinical decision support tool

Hans-Michael Tautenhahn^{1,2} | Tim Ricken^{*3} | Uta Dahmen¹ | Luis Mandl³ | Laura Bütow² | Steffen Gerhäuser³ | Lena Lambers³ | Xinpei Chen¹ | Elina Lehmann⁴ | Olaf Dirsch⁴ | Matthias König⁵

¹Experimental Transplantation Surgery,
Department of General, Visceral and
Vascular Surgery, Jena University Hospital,
Germany

²Department of General, Visceral and
Vascular Surgery, Jena University Hospital,
Germany

³Institute of Structural Mechanics and
Dynamics in Aerospace Engineering,

Faculty of Aerospace Engineering and
Geodesy, University of Stuttgart, Germany

⁴Institute of Pathology, Klinikum Chemnitz,
Germany

⁵Systems Medicine of the Liver, Institute for
Theoretical Biology, Humboldt University
Berlin, Germany

Correspondence

*Tim Ricken, Pfaffenwaldring 27, 70569
Stuttgart, Germany. Email:
tim.ricken@isd.uni-stuttgart.de

Summary

The SIMulation supported LIVER Assessment for donor organs (SimLivA) project aims to develop a mathematical model to accurately simulate the influence of mechanical alterations in marginal liver grafts (specifically steatotic ones) and cold ischemia on early ischemia-reperfusion injury (IRI) during liver transplantation. Our project tackles significant research challenges, including the co-development of computational methodologies, experimental studies, clinical processes, and technical workflows. We aim to refine a continuum-biomechanical model for enhanced IRI prediction, collect pivotal experimental and clinical data, and assess the clinical applicability of our model. Our efforts involve augmenting and tailoring a coupled continuum-biomechanical, multiphase, and multi-scale partial differential equation-ordinary differential equation (PDE-ODE) model of the liver lobule, allowing us to numerically simulate IRI depending on the degree of steatosis and the duration of ischemia. The envisaged model will intertwine the structure, perfusion, and function of the liver, serving as a crucial aid in clinical decision-making processes. We view this as the initial step towards an in-silico clinical decision support tool aimed at enhancing the outcomes of liver transplantation. In this paper, we provide an overview of the SimLivA project and our preliminary findings, which include: a cellular model that delineates critical processes in the context of IRI during transplantation; and the integration of this model into a multi-scale PDE-ODE model using a homogenized, multi-scale, multi-component approach within the Theory of Porous Media (TPM) framework. The model has successfully simulated the interconnected relationship between structure, perfusion, and function—all of which are integral to IRI. Additionally, we have been able to study the impact of tissue perfusion and temperature, two critical parameters in the context of liver transplantation.

KEYWORDS:

ischemia-reperfusion injury, IRI, liver transplantation, ODE, PDE, porous media

⁰**Abbreviations:** IRI, ischemia reperfusion injury; LTx, liver transplantation; ODE, ordinary differential equation; PDE, partial differential equation, SBML, systems biology markup language; SimLivA, SIMulation supported LIVer Assessment for donor organs; TPM, theory of porous media

1 | INTRODUCTION

Liver transplantation (LTx) remains the only curative intervention for acute and chronic end-stage liver disease. A prominent and as yet unresolved issue in the realm of transplantation medicine is the scarcity of donor organs. Over the previous decade, the discrepancy between the number of patients on the waiting list and the supply of available donor organs has been on the rise, as evidenced by statistics from Eurotransplant (<https://statistics.eurotransplant.org/>).

Demographic change and western lifestyle result in an increasing rate of elderly multi-morbid patients in need for liver transplantation. At the same time, there is a strikingly high rate of elderly, multi-morbid donor organs. Liver grafts from these donors, so-called marginal organs, are often affected by hepatic steatosis, significantly compromising the quality of the donor organ [24]. This reduced quality is largely due to alterations in tissue structure, leading to diminished organ perfusion and, subsequently, impaired hepatic function.

When presented with a marginal graft, the transplant surgeon is faced with the clinical decision of whether to accept or reject the organ for a given patient. Rejection may culminate in the death of the patient on the waiting list, while accepting the marginal graft considerably elevates the risk of postoperative morbidity and mortality for the recipient. This clinical decision must be taken in the time-critical phase between organ procurement and transplantation. This decision-making process involves three time-critical judgement points: (1) before procurement, (2) after procurement and (3) immediately before transplantation, cf. figure 1.

The process starts with the identification of the potential donor followed by organ procurement. Upon removal, the organ is stored in a cold storage solution throughout transport to the transplantation center, marking the cold ischemia time. Upon implantation and reconnection of the blood vessels, the cold-stored, energy-depleted organ undergoes reperfusion and reoxygenation, culminating in ischemia reperfusion injury (IRI) and resultant hepatic damage of indeterminate severity. Within 48 hours post-transplantation, the severity of IRI reaches its peak or may even advance to delayed graft function or primary non-function, serving as a prognostic indicator of graft and patient survival.

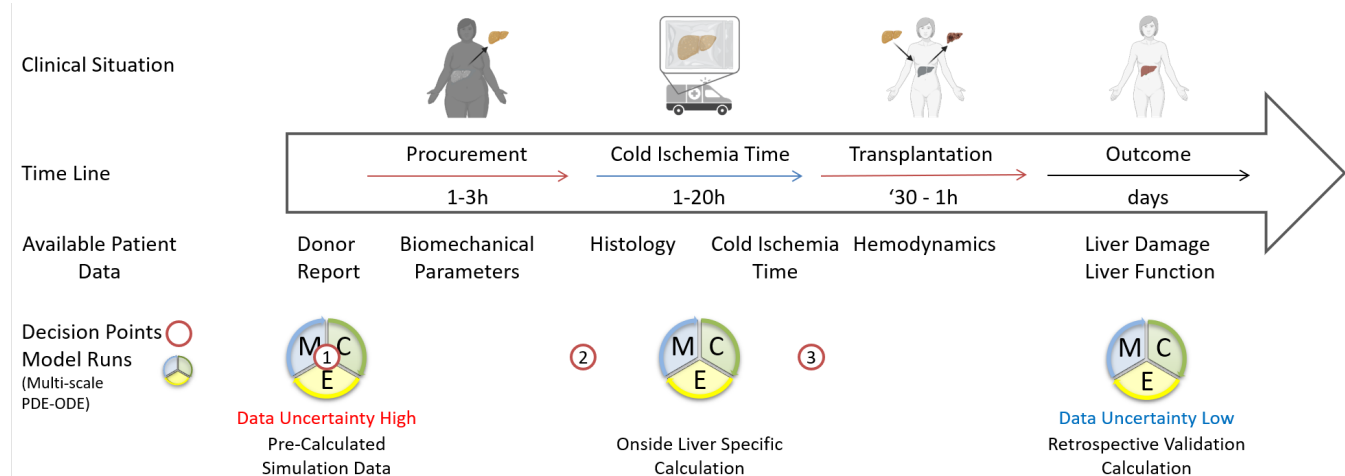


Figure 1 Flow chart of key steps of liver transplantation: i) Organ procurement. Donor condition (e.g. obesity) affects graft quality (e.g. hepatic steatosis). ii) Organ transport. Graft is stored in a cold preservation solution for the transport (cold ischemia time), leading to energy depletion and ischemic damage of unknown severity. iii) Organ transplantation. Reconnecting graft and recipient blood vessels initiates reperfusion and reoxygenation of the transplanted graft, resulting in IRI. iv) Outcome. Within 48h after LTx, severity of IRI (damage and function of the graft) can be assessed (delayed graft function/primary non-function), indicative of graft and patient survival. The three time-critical decision points to accept or reject a liver graft are (1) before procurement; (2) after procurement and (3) immediately before transplantation. Image created with Biorender.com.

2 | STATE-OF-THE-ART

2.1 | Cellular Scale

A critical factor for organ quality is the state and possible damage of liver cells following cold ischemia. At the cellular scale, dynamic processes relevant for IRI such as metabolism and signal transduction can be effectively modeled using ordinary differential equations (ODEs). Various models representing metabolic pathways pertinent to IRI have been constructed, cf. [37, 23, 33, 1, 28, 18, 19, 2]. These models can be conveniently encoded in the Systems Biology Markup Language (SBML) [11, 9], a format that facilitates model exchange, integration, and reproducibility. However, a noticeable gap persists in the development of ODE models that consolidate molecular processes essential for both IRI and steatosis.

An overview of mathematical models on the liver cellular scale can be found in [4], [30] and [20].

2.2 | Lobular Scale

A large number of mathematical and numerical models exist for the mathematical description of processes in the human body and especially in the liver. In this first models, hepatocyte, sinusoids, hepatic lobules, vascular system, and overall organ scales have been considered individually and decoupledly. RANI ET AL. [27] and DEBBAUT ET AL. [7] both provide pure fluid dynamic models for the description of blood microperfusion without taking into account metabolism. However, because of how directly metabolism is impacted by gradients created by metabolic activity, metabolic function is connected to blood perfusion. Additionally, there are differences in the hepatocytes' metabolic characteristics throughout the sinusoids (a process known as metabolic zonation), with periportal and perivenous hepatocytes displaying distinct metabolic capacities that are crucial for steatosis and oxidative damage [10]. To map the matching zonation pattern in silico, general one-dimensional sinusoidal models were created; see [2]. The two-dimensional model provided by [3] to describe the blood flow driven convection-reaction mechanism is an extension to the general one-dimensional sinusoidal model. This study discusses a microcirculatory networks technique.

While cellular models excel at simulating time-dependent modifications and interactions at a cellular scale, such as during fat accumulation or oxidative stress, they fall short in representing elastomechanical properties at the tissue scale, including, for example, the poroelastic structural behavior of liver tissue. In conditions such as hepatic steatosis, an increased pressure resistance emerges due to cellular fat accumulation. This subsequently results in reduced sinusoidal perfusion, influencing the nutrition and oxygen supply to the hepatocytes, impacting metabolism, e.g. affecting the turnover of triglycerides. Consequently, liver function becomes closely tied with perfusion, structural alterations due to pathology, and ensuing tissue stress and strain.

In order to map the multidimensional coupled relationship between structure, perfusion and function, RICKEN, DAHMEN and KÖNIG proposed a coupled PDE-ODE model, see [32, 21, 39]. It is based on a homogenized multi-scale multi-component approach in the framework Theory of Porous Media (TPM). Coupled PDEs were used to simulate deformation, flow and growth processes as well as advection-diffusion reaction processes in blood. In order to consider the metabolic processes on the cell scale, this model was coupled with ODE-metabolism models of KÖNIG[18] and SCHLEICHER [33]. With this in hand, a comprehensive high-fidelity model became available, which is in principle able to represent all essential scales and effects of IRI.

To encapsulate the intricate relationship between structure, perfusion, and function, RICKEN and KÖNIG proposed a coupled model of partial differential equations (PDEs) and ODEs, as discussed in [32, 21, 39]. This model leverages a homogenized multi-scale, multi-component methodology within the TPM framework. It utilizes coupled PDEs to simulate deformation, flow, growth, and advection-diffusion reaction processes in blood. To incorporate the metabolic processes at the cellular scale, this model was integrated with the ODE-metabolism models developed by KÖNIG [18] and SCHLEICHER [33]. This approach has yielded a comprehensive, high-fidelity model that is, in principle, capable of representing all essential scales and effects of IRI.

An overview of mathematical models on the liver lobular scale can be found in [4] and [30].

2.3 | Model Coupling

Kinetic models of cellular metabolism (ODE) have to be coupled with elasto-mechanical models of the liver lobulus (PDE) in order to characterize the multi-scale pathophysiological processes in IRI, which include cellular processes, perfusion, as well as the elasto-mechanical properties of the tissue. Therefore, the PDE system includes transport and poro-elastic tissue characteristics and receives source and sink terms from reactive steps defined in the metabolic pathways models. This process of PDE-ODE coupling can be seen in KÖPPL [16], PALINACHAMY [25] or RICKEN[32]. In PDE-ODE coupling a distinction is made between two main coupling strategies. On the one hand the PDE-ODE system is solved using a PDE solver. This solution

approach has the drawback of slow calculation times, especially when large ODE systems, such as metabolic pathways, must be added in many PDE grid points. Furthermore, it involves the overhead of transforming the ODE system for the appropriate PDE framework. On the other hand, model order reduction (MOR) methods can be used to reduce the dimensionality of the PDE, ODE or both systems and hence improve the effectiveness of the numerical solution.

Furthermore, coupling of different models with various model interfaces requires standardization, especially if the models contain different modeling frameworks (ODE and PDE) or multiple scale (whole body, lobule, cell). Here, Systems Biology Markup Language (SBML) [9, 11] serves as the de facto standard representation for description and exchange of cellular ODE models. Extensions to SBML have been developed for model coupling based on hierarchical model composition, cf. [35]. However, the connection of ODE models to porous media (PDE-ODE) is not yet existing in standard formats or interfaces and therefore would be a significant extension.

2.4 | Clinical Situation

Currently, liver transplantation is the gold standard for treating end-stage liver disease. The majority of organ transplants nowadays are performed using less-than-ideal (marginal) donors. Many of them already have fatty liver disease, as a result of demographic change and western lifestyles. The transplant physician must take a decision whether to accept these borderline organs and running the risk of organ dysfunction or to reject the specific organ and running the chance of the patient dying while on the waiting list. Furthermore, this decision must be taken under time constraints, when not necessarily all required information of the donor and recipient are available. Fatty liver disease, and here especially macrosteatosis results in the enlargement of the hepatocyte with leads to narrowing of the liver capillaries, the so-called sinusoids. This in return affects the poroelastic characteristics (vessel radius and pressure, organ stiffness) and the perfusion of the liver. Impaired liver perfusion and inhomogeneous microcirculation brought on by this structural alteration in the sinusoids worsen the metabolic dysfunction of the steatotic liver graft. As a result energy and carbohydrate/lipid (CH/L) metabolism and the production of reactive oxygen species (ROS) [5, 26] are affected. Ischemia time is the second important factor impacting organ function following transplantation, in addition to these restrictions imposed by the donor organ. Massive lipid peroxidation is started by IRI, which sets off a vicious cycle. Hepatocyte damage and eventual death are caused by the ROS that are produced during the process of preperfusion. Taken together, IRI impairs metabolic processes, which affect the entire organ and may cause hepatic dysfunction or possibly liver failure. It is not yet known with certainty how steatosis and ischemia time in IRI are quantitatively related. The numerous, intricately intertwined pathophysiological processes involving blood flow, cellular functions (oxidative stress, energy metabolism), and mechanical qualities of the tissue are making the prediction rather difficult. The decision-making process could be facilitated by a clinically usable in silico decision tool that considers the intricate interplay between the mechanical properties of the (steatotic) graft, hepatic perfusion, and the metabolic impairment caused by the underlying steatosis of the graft.

3 | SIMLIVA PROJECT OVERVIEW

The goal of our project "SIMulation supported LIVer Assessment for donor organs (SimLivA)" is to mathematically model the impact of mechanical alterations of the (steatotic) marginal liver graft and cold ischemia on early IRI. The project combines mechanical and systems biology modeling with clinical data and experimental studies. On the modelling side, we adapt and improve our coupled continuum-biomechanical multi-phase and multi-scale model of the liver lobule, a coupled system of PDEs and ODEs. Parameterization and validation of the model is based on animal and human data. Taking into account the interplay between mechanical properties of the graft, hepatic perfusion and the affected molecular pathways provides an in-silico clinical decision support tool for decisions pro or contra the marginal organ by predicting hepatic damage and early graft function. In the following we describe the underlying concepts for multi-scale modeling, clinical and experimental data acquisition as well as our image analysis pipeline to include information from clinical image data of routine examinations into the modeling approach. The overall scheme, as illustrated in figure 2, shows the incorporation of animal and human data to reflect initial donor organ quality (e.g. steatosis), cold ischemic damage, and early IRI.

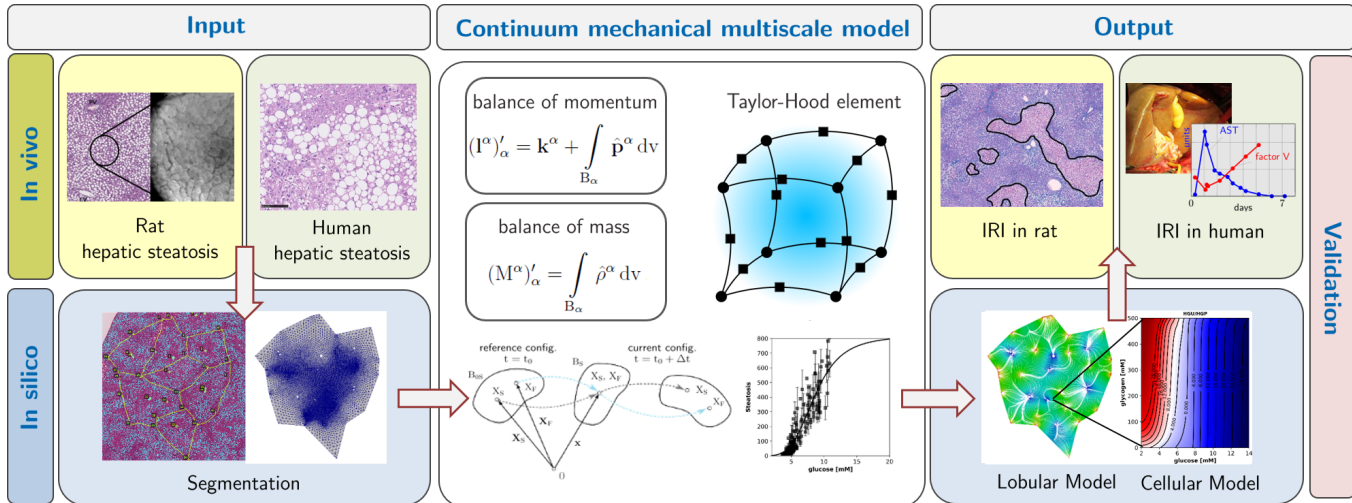


Figure 2 Co-design of modeling, animal experiments, and clinical evaluation within SimLivA to predict the impact of steatosis-induced mechanical alterations and cold ischemia on early IRI in the marginal liver graft. The continuum-mechanical PDE-ODE model of the liver lobule is parameterized based on animal and human data. IRI is predicted by models tailored to the respective data sets and evaluated against animal and human data.

3.1 | Modelling Concept

The underlying modeling concept (cf. figure 2) can be divided into lobule-level modeling, cell-level modeling, and interconnecting multi-scale coupling. While the individual components are presented in the following chapters in relation to their subject disciplines, we will first present the overall concept to appropriately investigate the essential phenomena for the prediction of early IRI depending on steatosis degree and the duration of ischemia. For this purpose, the PDE system at the lobule level provides the deformation-advection-diffusion-reaction equation to account for solute transport, such as oxygen and nutrients, and structure-perfusion remodeling based on a homogenised multiphase model derived using the TPM. Furthermore, at the cellular level, the ODE system determines CH/L metabolism and oxidative damage depending on steatosis and nutrient availability. The ODE models will be encoded in systems biology markup language (SBML). Based on this, we combine standardized ODE models and PDE models to obtain a coupled multi-phase and multi-scale model to obtain a reliable prediction of ischemic damage and severity of IRI.

3.1.1 | Modelling on Lobular Scale

The model of the liver lobule based on the TPM can be split into a general model describing general phenomena in the lobule as well as a specialized model to account for changes to model IRI. As we use a homogenized model, blood flow through sinusoids is described by a transversal-isotropic microperfusion. The sinusoidal structure and direction itself is developed in response to the pressure and its respective changes [29]. Also included is the poro-elastic deformation of liver tissue. Further, the general model describes poro-elastic coupling with perfusion, diffusive-advective transport of metabolically relevant substances dissolved in blood, such as glucose, lactate, free-fatty acids, and oxygen [32]. Similarly, the influence of different pressure gradients between portal triad and central veins in connection with nutrient transport on cell metabolism can be calculated. To account for IRI and LTx, we describe the relevant phases by a tetraphasic model consisting of liver tissue, fat, necrotic tissue, as well as a fluid phase describing blood or the preservation solution, depending on the point of time. Herein we describe the diffusive-advective transport of oxygen and other metabolites, i.e., glucose and lactose, in the fluid. The reaction rates from the cell model are incorporated into the lobule model as changes in the volume fractions and concentrations of the tissue. Further information on the fundamental model using the extended TPM (eTPM) can be found in the work of LAMBERS [20]. We use FEBio [22] to solve the equation system on the lobular scale with the finite element method.

To account for IRI during LTx, we start by applying normal perfusion and nutrient supply within the organ donor. In this approach, we describe the phase of cold ischemia by an exchange of the fluid phase from blood to a nutrient solution, a decrease in temperature from 37°C to 4°C, and a cessation of perfusion through the organ and thus the underlying vascular structure.

Corresponding to this is then the change in the mechanical properties of the fabric (stiffening) based on the aforementioned changes. After the end of cold ischemia and successful implantation, the organ and lobules are then perfused with blood again and brought to body temperature. The built-up contaminants and metabolites are then transported back through the lobule potentially inducing additional damage. This allows for assessment of the influence of reperfusion on stiffness, perfusion, and metabolism. Furthermore, we can evaluate the influence of different types and distributions of steatosis on pressure gradients from portal to central vein.

3.1.2 | Modelling on Cellular Scale

To date, only simplified models of glucose and fat metabolism have been interfaced with the porous media approach [32, 31]. These models can predict glucose metabolism and fat accumulation within the liver lobule. However, the existing simplified cellular models do not incorporate spatial heterogeneity. The cellular ODE model will be extended to describe CH/L metabolism with particular emphasis on fat accumulation, integrated with the ischemic damage (ROS) under nutrient depletion (oxygen and glucose) and degree of steatosis. The model will incorporate cell damage and necrosis resulting from ROS and nutrient depletion. To facilitate coupling, the model will be encoded in Systems Biology Markup Language (SBML) [11, 9].

Informed by spatially resolved animal and human data derived from liver histologies (for instance, fat content, key enzymes, and oxidative damage markers), we will generate individualized, spatially resolved liver lobule models. Depending on their spatial position and corresponding data (in a zonated model), the integrated cellular model will be parameterized variably. This necessitates the development of robust cellular ODE models capable of operating across a wide array of parameter combinations, with allowances for model uncertainties. By implementing parameter scans and sensitivity analyses, we will thoroughly investigate the input-output behavior of the ODE models. We will utilize the following animal and human data for model parameterization and validation: (i) clinical chemical parameters (ALT, AST, GGT, LDH, CHE, albumin, bilirubin) as indicators of cell damage and necrosis; (ii) histology-derived fat and glycogen content; (iii) histological HIF-1alpha as a proxy for oxygen depletion; (iv) HNE, catalase (CAT), glutathione peroxidase (GPX) and superoxide dismutase (SOD) as markers for oxidative damage; (v) glucokinase (GK), pyruvate kinase (PK) and phosphofructokinase (PFK) as indicators of glycolytic capacity.

3.1.3 | Multi-Scale Coupling

A crucial task entails the expansion and standardization of existing coupling mechanisms for the robust integration of models operating on different scales—specifically, the connection between tissue-level PDE models and cellular ODE models. This requires implementing the standard exchange format SBML for ODE-PDE coupling and developing the corresponding PDE-ODE interfaces based on these standards. For instance, the transport rates of ODE boundary species serve as sources and sink terms in the porous media approach. All cellular models will adopt SBML encoding, with interfaces for model coupling facilitated through SBML hierarchical model composition, which includes annotations of ports, units, and conversion factors. This strategy fosters an agile modeling workflow, enabling immediate updates to the coupled PDE-ODE model following modifications to either the ODE or PDE model. Additionally, utilizing a recognized exchange format for ODE models ensures the reproducibility of results, along with the reusability and extensibility of our PDE-ODE coupling methodology.

An important part for the PDE-ODE coupling is an efficient and correct numerical solution of the multiple ODE problems (a full kinetic model has to be solved at every grid point), even for stiff ODE systems. Within a proof-of-principle, we integrated the co-developed high-performance SBML solver roadrunner [36, 38] into a continuum-biomechanical TPM model of the liver within FEBio [22] as shown in figure 3. The coupling of the solvers will be formalized and standardized. This will also ensure correctness of implementation of the ODE part, because the identical (and due to SBML reproducible) solver will be used for isolated ODE simulations and coupled PDE-ODE simulations. Efficient and accurate numerical solutions of multiple ODE problems constitute a vital component of PDE-ODE coupling—even for stiff ODE systems. As part of a proof-of-principle, we integrated the high-performance SBML solver roadrunner [36, 38] into a continuum-biomechanical TPM model of the liver. A common issue in model coupling is the potential for errors during model translation when interfacing with a different framework, such as typos in kinetic equations, unit discrepancies, or varying syntax of programming languages. By employing the same SBML model encoding and identical ODE simulator for both the isolated ODE and coupled PDE-ODE models, these issues can be mitigated, resulting in robust coupling. This approach ensures the correct implementation of the ODE component, as the identical (and thus, due to SBML, reproducible) solver will be used for both isolated ODE simulations and coupled PDE-ODE simulations.

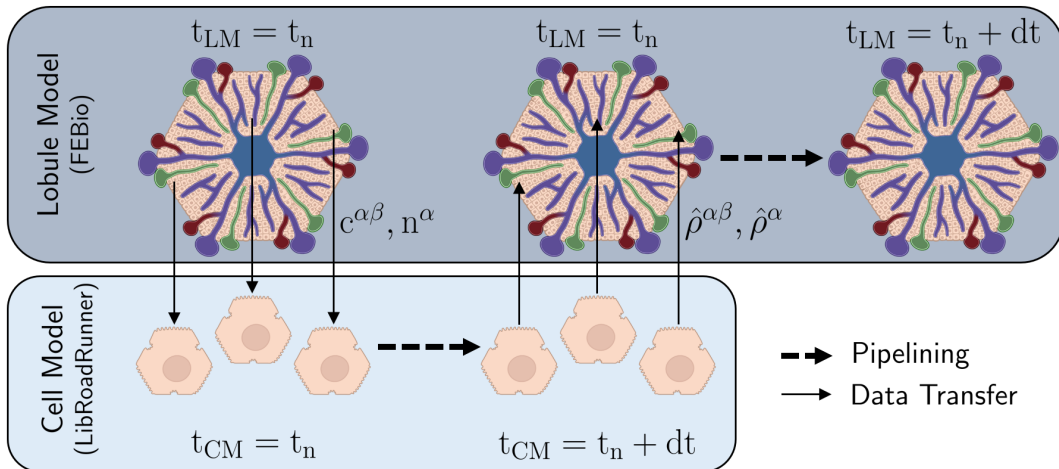


Figure 3 Coupling scheme of cell model (CM) using the SBML solver roadrunner [36, 38] and FEBio [22] for the lobule model (LM). At the current time step, the solute concentrations ($c^{\alpha\beta}$) and volume fractions (n^α) in each Gauss point are passed to the respective cellular model. Then a timestep of dt is performed on cellular scale, resulting in the respective source and sink terms ($\hat{p}^{\alpha\beta}$ and \hat{p}^α) which are passed to the lobule model. Those are then included in the time step performed within FEBio. The phases α are solid tissue and fluid phase, while the solutes β are glucose, oxygen, and lactate.

In addition, we aim to establish model interfaces between computational models and clinical applications, as well as between animal and human data and models. By precisely defining all input and output formats, we can ensure robust data integration of human and animal data into our models.

3.2 | Experimental and Clinical Data

An important goal of the project is to accumulate crucial data for model parameterization and validation. We intend to quantify the changes induced by steatosis in terms of structure, perfusion, hepatic metabolism, and hepatic damage, as well as the resultant influence on hepatic IRI. In order to estimate the structure and the degree of hepatic steatosis and to get a first overview of the liver zonation, hematoxylin-eosin (HE) stains of animal and human liver samples are prepared and used for modeling, see section 3.3.

Even donor organs macroscopically judged to be functionally good, may show severe microsteatosis in histology and impaired liver function after transplantation as visible in figure 4a. Almost every hepatocyte is affected by microsteatosis. Furthermore, zonally accentuated macrosteatosis can be observed (figure 4a right). In particular, marcosteatosis leads to impairment of the sinusoids, which ultimately results in an influence on perfusion via the sinusoids. Figure 4b shows the diameter narrowing of the sinusoids due to lipid droplet deposition (figure 4b white arrow). The patient showed a graft failure, therefore a listing for re-transplantation, seven days after the operation, followed. For the detailed evaluation of hepatic zonation, immunohistological images of typical functional zonation markers are obtained from both human liver samples and experimental rat liver samples. An important pericentral marker is glutamine synthetase, which is distinctively localized in the first cell layers around the central vein.

The estimation of metabolic liver capacity will be performed by histological and functional evaluation of selected cytochrome P450 isoenzymes (especially CYP3A4 and CYP1A2, cf. figure 4c).

In addition to the morphological analysis and characterization of metabolic function, liver synthesis capacity is determined, measuring albumin and factor v in blood samples. Also a comprehensive LiMAX test as a current clinical standard diagnostic for addressing liver function is conceivable. In order to map the hepatic damage, the staining and evaluation of the inflammatory mediator HMGB1 is performed, and DNA damage, caused by the ROS production, is detected by means of 8-hydroxydeoxyguanosine (8-OHdG).

We also aim to assess the clinical applicability of SimLivA. This includes scrutinizing the technical workflow with respect to data management, computational resources, processing speed, and data security. Additionally, we will measure clinical usability by evaluating its practicality, intuitive operability, and time expenditure. We plan to refine the clinical pathway based on

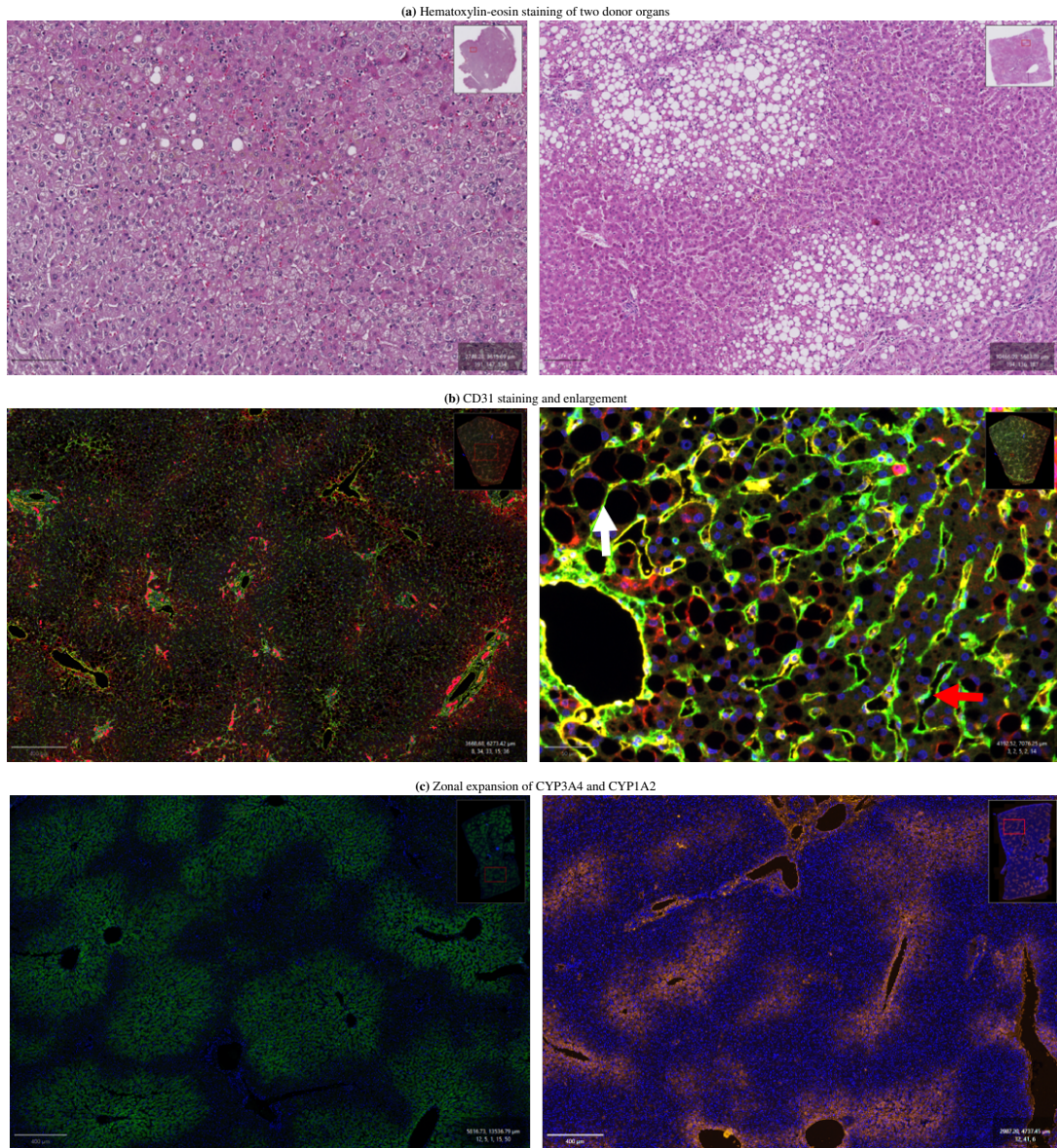


Figure 4 Donor organs have different degrees of lipid incorporation, this is shown by HE overviews of two donor organs in subfigure A. Sinusoids can be detected by CD31 as shown in subfigure B. In the enlargement, impairment of sinusoidal diameter (white arrow) by lipid droplet incorporation into two adjacent hepatocytes, in contrast an unaffected sinusoidal diameter (red arrow) can be evaluated. subfigure C shows histological estimation of metabolic capacity by zonal expansion of CYP3A4 (green) and CYP1A2 (red).

predictions made using the co-designed model and carry out a prospective proof-of-concept study to evaluate the reliability of the model-based predictions.

We will assess how steatosis-induced changes in structure, perfusion and metabolism influence early IRI. For this purpose, we have selected a set of parameters that reflect donor organ quality, ischemic damage and early IRI. These factors addressing metabolic function, morphological changes and injury markers. Animal experiments are essential to collect data under standardized conditions, which represents a simplification of the clinical situation. We aim to align the data acquisition from animals and humans as closely as possible.

Human data will be obtained and used in three different ways: prospective data collection, analysis of archived data and clinical proof of concept. We plan to acquire data from 45 clinical transplantation procedures. Doing so we will include donor

organs with steatosis of various severity ranging from healthy to moderately steatotic donor organs. The donor organs will be subjected to different cold ischemia times ranging between 30 min and 12 hours caused by the respective allocation process.

Clinical data will be extracted from the donor organ report and the charts of the recipient. Whenever clinically possible, we will obtain tissue samples from the donor during operation, first from the cold stored graft at the end of cold ischemia and second from the recipient after reperfusion (time-zero-biopsy). Due to the variable surgical situation there are differences in the ischemia and reperfusion time. The intraoperative dynamic assessments of the liver organ will be performed in the recipient only due to the time constraints during organ procurement.

We will evaluate the clinical usability of SimLivA in terms of practicability, intuitive operability, and time expenditure. We will perform a prospective proof of concept to evaluate the reliability of the model-based predictions using the limited available donor data within the given time constraints. In this proof of concept we want to test the following workflow: (1) The transplant pathologist receives the donor organ report together with the whole slide scan of the liver biopsy; (2) The pathological diagnosis based on the biopsy is communicated to the DSO; (3) The surgeon decides about the use of the organ and records his preliminary decision; (4) In the meantime, the pathologist will upload the donor organ report together with the whole slide scan and the expected cold ischemia time to SimLivA; (5) Using the clinical data as model input, the SimLivA graft assessment is performed and an IRI-severity simulation report depending on ischemia time is created (including uncertainties); (6) The results are transferred to the transplant surgeon who can re-evaluate his decision. We aim to determine the extent to which the SimLivA results aid the surgical decision and accurately predict the postoperative course.

3.3 | Image Analysis

In order to process the resulting histological data, i.e., HE stained slides, a semi-automatic image processing routine is applied. This segmentation and (zonated) quantification is then used as direct input for model parameterization (e.g. spatial geometries, distribution of fat) as well as a support for the clinical side shall be supported by providing more information than a classical pathological report. For automatic instance segmentation of hepatocytes and vessels, we use Mask-R-CNNs [8]. For hepatocytes, we defined 12 classes, which are composed of variations in the number of visible nuclei (0, 1, 2 & more), as well as type of steatosis of the respective hepatocyte (no steatosis, micro-, medio-, or macrovesicular steatosis). The vesicular structure is represented by portal fields and central veins which, as single entities, complete the identified classes. Subsequently, individual lobules will be identified in a post-processing step (cf. [34]) which allows the extraction of zonated information.

This will not only allow us to transfer the steatosis information into the porous media model in form of volume fractions, but through the cell-based counting approach we emulate the gold standard of counting methods in pathology. As additional information on organ quality, the number of cell nuclei can be used to estimate the cell division rate.

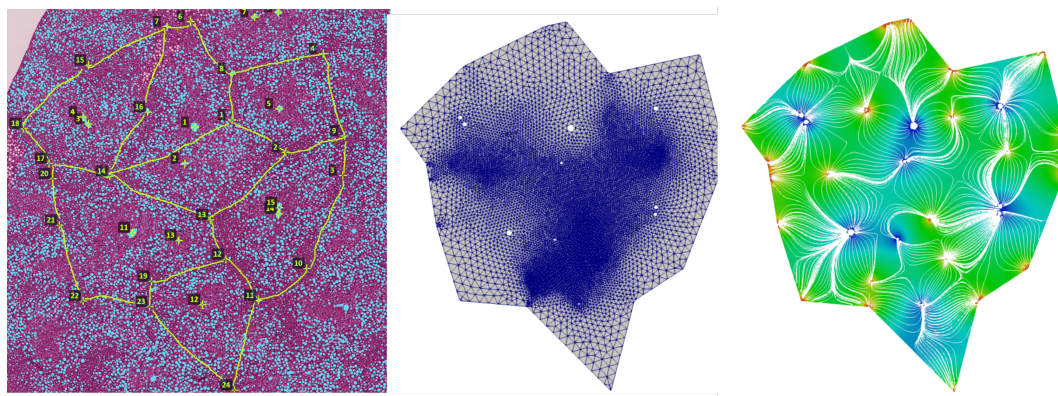


Figure 5 Semi-automatic segmentation of liver lobule geometry with inflow at the portal triads. a) Manually segmented liver lobules using a histological image of steatotic rat liver, b) meshed geometry obtained through a meshing tool, c) simulation results showing the pressure distribution as well as stream lines representing the blood flow from periportal triads to the central veins.

4 | RESULTS

In the following sections we present preliminary results, which include: a cellular model that delineates critical processes in the context of IRI during transplantation; and the integration of this model into a multi-scale PDE-ODE model using a homogenized, multi-scale, multi-component approach within the TPM framework. The model was applied to successfully simulate the interconnected relationship between structure, perfusion, and function—all of which are integral to IRI. Additionally, we have been able to systematically study the impact of temperature and ischemia time, two critical parameters in the context of liver transplantation.

4.1 | Cellular model

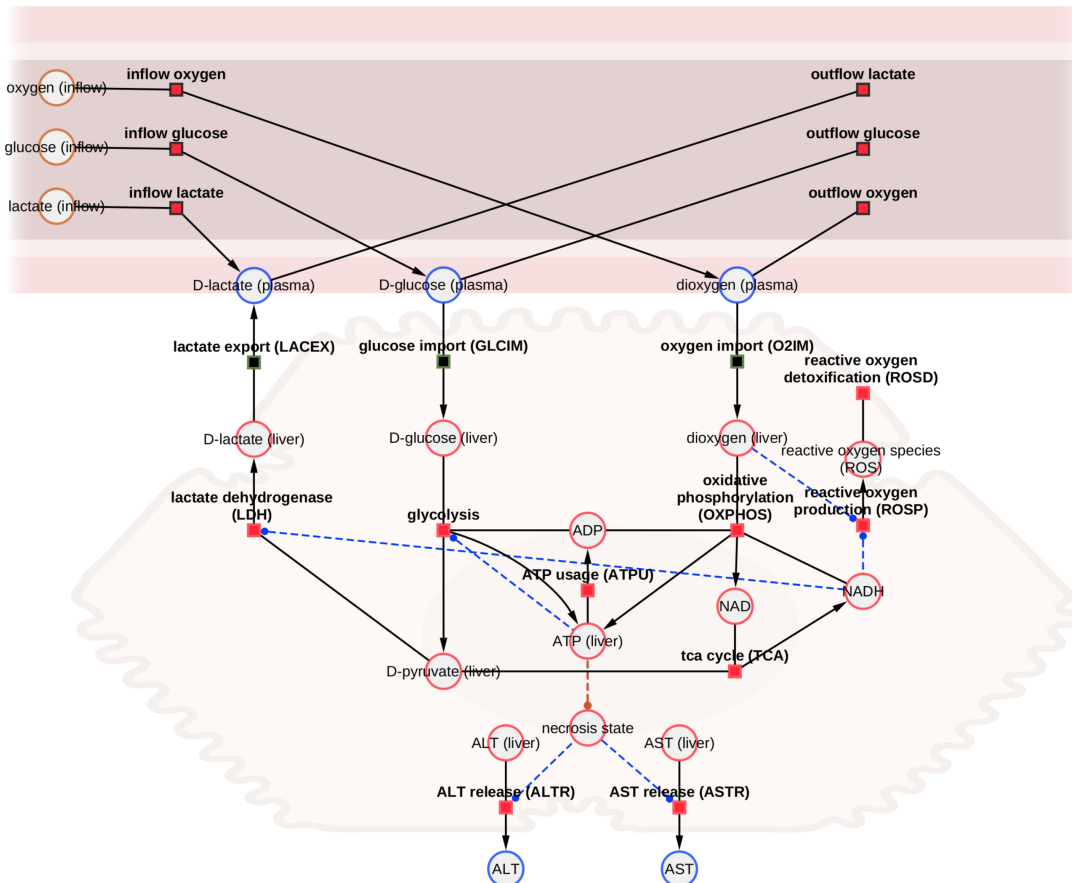


Figure 6 Overview of a cellular model illustrating the processes involved in IRI. The depicted interactions show how glucose, lactate, and O₂ can be exchanged between the plasma (liquid) phase and hepatocyte (solid) phase. Glucose is converted into pyruvate through glycolysis, generating ATP from ADP in the process. Subsequently, pyruvate can either be converted to lactate under anaerobic conditions or undergo oxidation in the TCA cycle to generate reduced redox equivalents, namely NADH. NADH, in an oxygen-rich environment, can further be utilized in the process of oxidative phosphorylation to create ATP. A severe drop in ATP levels can lead to cellular death or necrosis, ceasing all metabolic processes and subsequently releasing ALT and AST proteins from the cell. Additionally, in conditions of low oxygen concentration, the production of ROS can occur due to the absence of oxygen as a terminal electron acceptor in the electron transport chain. This cellular model is further connected to a simple perfusion model representing the inflow and outflow of glucose, oxygen, and lactate to simulate IRI using an ODE approach. All metabolic processes depicted are temperature-dependent, as detailed in the accompanying text. Created with BioRender.com and Cytoscape.

We developed a cellular model to describe key processes and events relevant in the context of IRI (figure 6). The model consists of the main energy reactions either via glycolysis of glucose to create ATP or oxidative phosphorylation. Glycolysis involves the conversion of glucose into pyruvate, releasing energy that is stored in the form of ATP (adenosine triphosphate) and NADH (nicotinamide adenine dinucleotide). In total, glycolysis results in a net gain of 2 ATP molecules, 2 NADH molecules, and 2 pyruvate molecules per molecule of glucose. Glycolysis does not require oxygen, which makes it an anaerobic process. However, the fate of the end product, pyruvate, depends on whether oxygen is present or not. In the presence of oxygen, pyruvate can undergo further oxidation in the mitochondria through the citric acid cycle (TCA cycle), while in the absence of oxygen, pyruvate undergoes conversion to lactate. During the oxidation of pyruvate in the TCA cycle reduced redox equivalents (NADH) are generated, from which energy in the form of ATP can be generated via oxidative phosphorylation using oxygen. In conditions of low oxygen concentration, the production of ROS can occur due to the absence of oxygen as a terminal electron acceptor in the electron transport chain.

Cell necrosis is a form of cell injury which leads to the premature death of cells in living tissue. It's characterized by the swelling of the cell, the rupture of the cell membrane, and subsequent spillage of cell contents into the surrounding tissue. Necrosis can occur as a result of factors such as insufficient energy (ATP). A severe drop in ATP levels can lead to cellular death or necrosis, ceasing all metabolic processes and subsequently releasing hepatic proteins such as alanine transaminase (ALT) or aspartate transaminase (AST) from the cell.

An important factor for the liver transplant is the temperature under which the organ is stored. To model the temperature dependence of the reaction rates and processes the following temperature dependence was added to all cellular processes.

$$f_{Ea} = 12.0 \quad [-]; \quad R = 8.314 \quad [\frac{\text{kg} \cdot \text{m}^2}{\text{s}^2 \cdot \text{mol} \cdot \text{K}}]; \quad T_{ref} = 310.15 \quad [\text{K}];$$

$$f_T(T) = \frac{e^{-\frac{f_{Ea} \cdot R \cdot T_{ref}}{R \cdot T}}}{e^{-\frac{f_{Ea} \cdot R \cdot T_{ref}}{R \cdot T_{ref}}}} = e^{f_{Ea}(1 - \frac{T_{ref}}{T})} \quad [-] \quad (1)$$

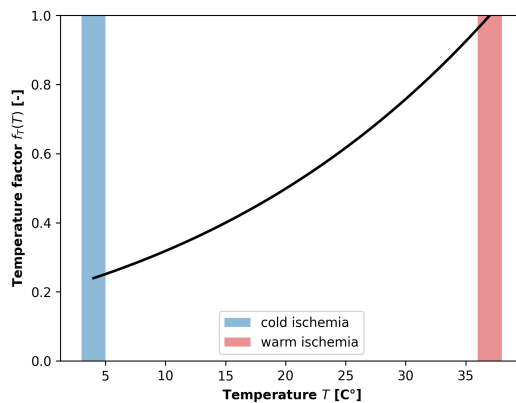


Figure 7 Temperature dependence of the metabolic processes $f_T(T)$. With decreasing temperature all metabolic processes slow down.

All reaction rates were made temperature dependent by multiplying with $f_T(T)$. The effect of the temperature on the reaction rates is depicted in figure 7. All metabolic processes slow down by around a factor of 5 under cold ischemia conditions compared to warm ischemia conditions ($T = 4^\circ\text{C} = 310.15\text{K}$, $f_T(277.15\text{K}) = 1.0$).

The resulting model allows to model key processes involved in IRI such as the temperature dependence of damage and ROS in the context of ischemia.

The model was encoded in the Systems Biology Markup Language (SBML) [11, 9], and developed using sbmlutils [13], a collection of Python utilities for building SBML models, and cy3sbml [14, 15], a visualization software for SBML. The model is an ODE model which is numerically solved by sbmlsim [12] based on the high-performance SBML simulator libroadrunner [36],

38]. The model is available under the CC-BY 4.0 license at <https://github.com/mattiaskoenig/iri-model>. Version 0.5.0 was used in this paper [17].

4.2 | Simulation of warm and cold ischemia

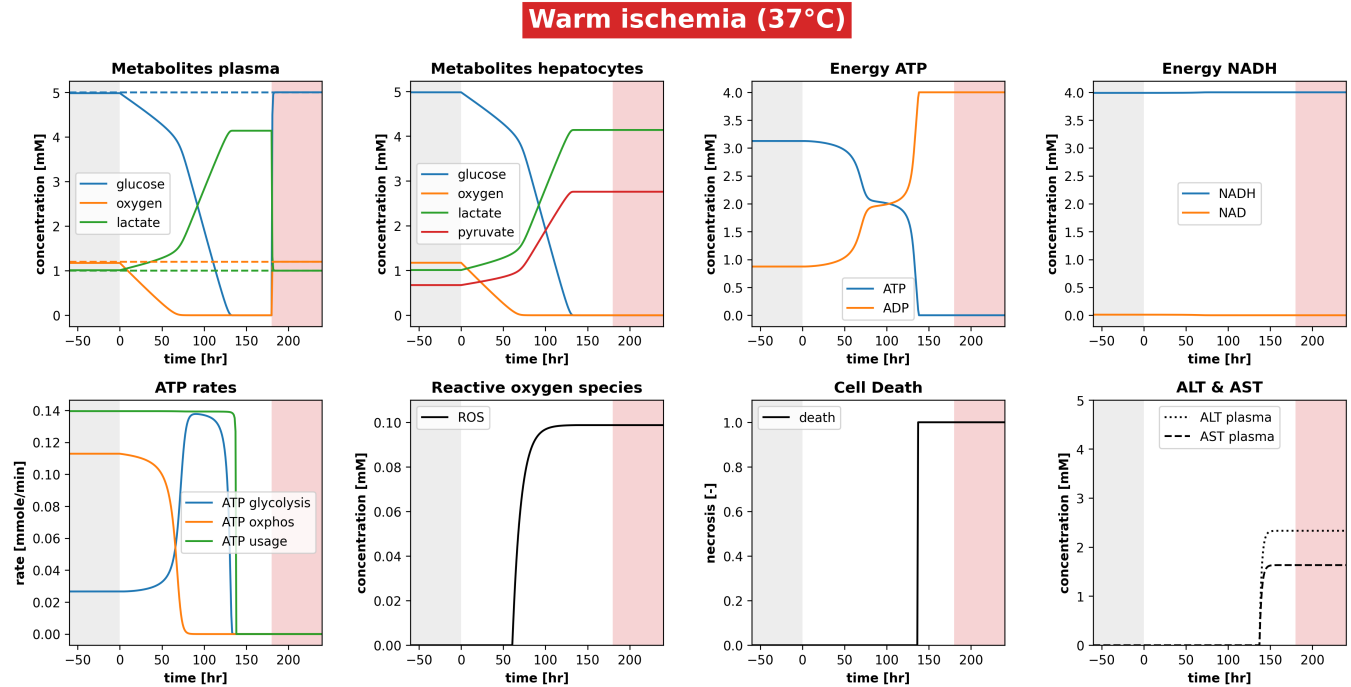


Figure 8 Warm perfusion-ischemia-reperfusion at 37°C (ODE perfusion model). After an initial steady state under the given perfusion conditions at 37°C is reached (grey area), perfusion is stopped from 0 min to 180 min resulting in ischemia at 37°C (white area), at which point reperfusion is started (red area).

The integration of a cellular model with a simple ODE perfusion model facilitated the simulation of perfusion-ischemia-reperfusion effects on hepatic metabolism and critical processes implicated in ischemia. These simulations were executed under warm ischemia conditions (with a temperature of 37°C or 310.15 K) and a 180-minute ischemia period (as shown in figure 8), as well as under cold ischemia conditions (at 4°C or 277.15 K) over the same ischemia duration.

During warm ischemia (figure 8), oxygen is rapidly exhausted within the first 60 minutes. Glucose levels initially decrease gradually while ATP can still be synthesized oxidatively; however, once oxygen is exhausted, glucose levels also deplete within the subsequent hour. This depletion corresponds with an abrupt rise in lactate due to anaerobic glycolysis, as pyruvate can no longer be oxidized within the TCA cycle. ATP levels remain steady as long as sufficient oxygen is present but fall to lower levels during anaerobic glycolysis. Following the consumption of all available glucose, the hepatocyte is unable to maintain ATP levels, leading to cell death and the subsequent release of ALT and AST. Concurrently, the absence of oxygen triggers the formation of reactive oxygen species.

Conversely, during cold ischemia (figure 9), metabolic processes are substantially decelerated, leading to a slower consumption rate of oxygen and glucose during ischemia. This allows the liver tissue to endure ischemic conditions for a more extended period. Consequently, ATP levels remain high, and no reactive oxygen species are formed within the initial 3 hours of cold ischemia.

To systematically investigate the influence of ischemia duration and temperature, we adjusted the temperature within a range of 1°C to 42°C and the ischemia duration from 1 minute up to 420 minutes (as shown in figure 10). As both temperature and ischemia duration escalated, there was a noticeable decrease in glucose and oxygen levels, alongside an elevation in lactate levels. This depletion in oxygen and glucose under conditions of high temperature and prolonged ischemia correlated with a

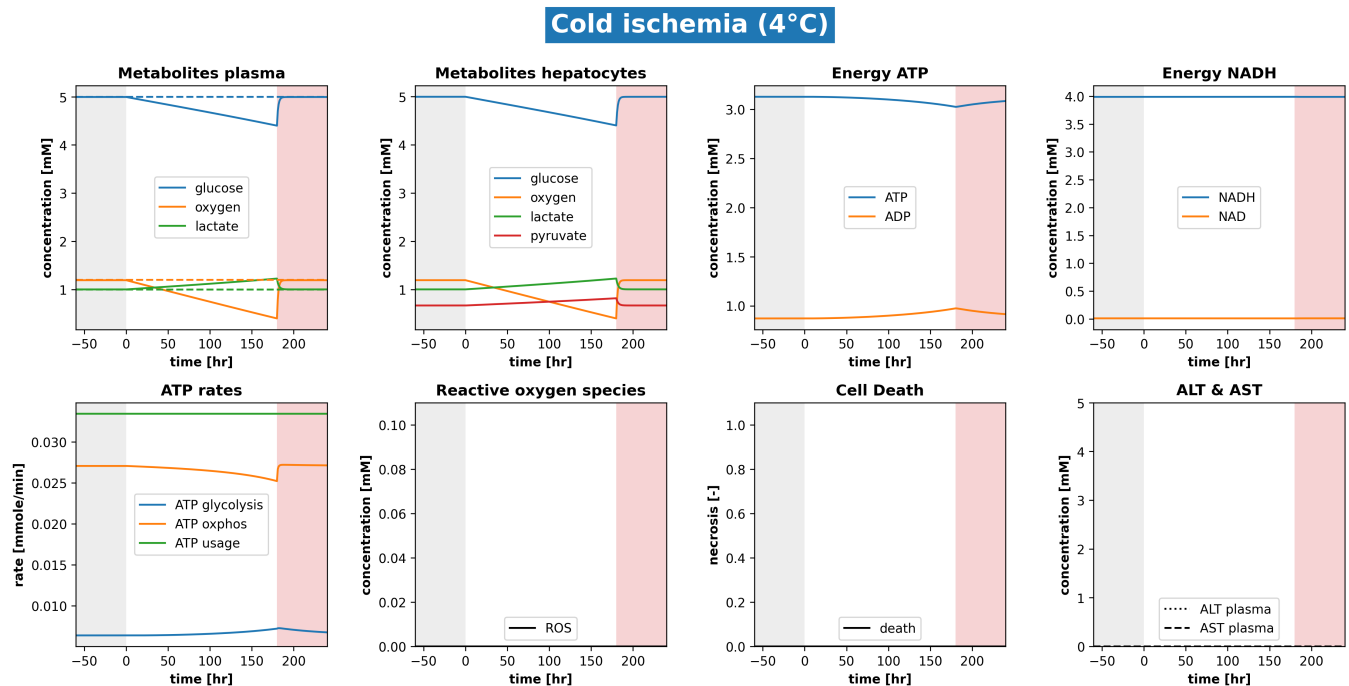


Figure 9 Cold perfusion-ischemia-reperfusion at 4°C (ODE perfusion model). After an initial steady state under the given perfusion conditions at 37°C is reached (grey area), perfusion is stopped from 0 min to 180 min resulting in ischemia at 4°C (white area), at which point reperfusion is started (red area).

significant reduction in ATP levels. Concurrently, there was an observed increase in the formation of ROS and necrosis, as well as the release of ALT and AST. Therefore, both the temperature and the duration of ischemia during liver transplantation emerged as critical factors in determining the quality of the transplanted organ.

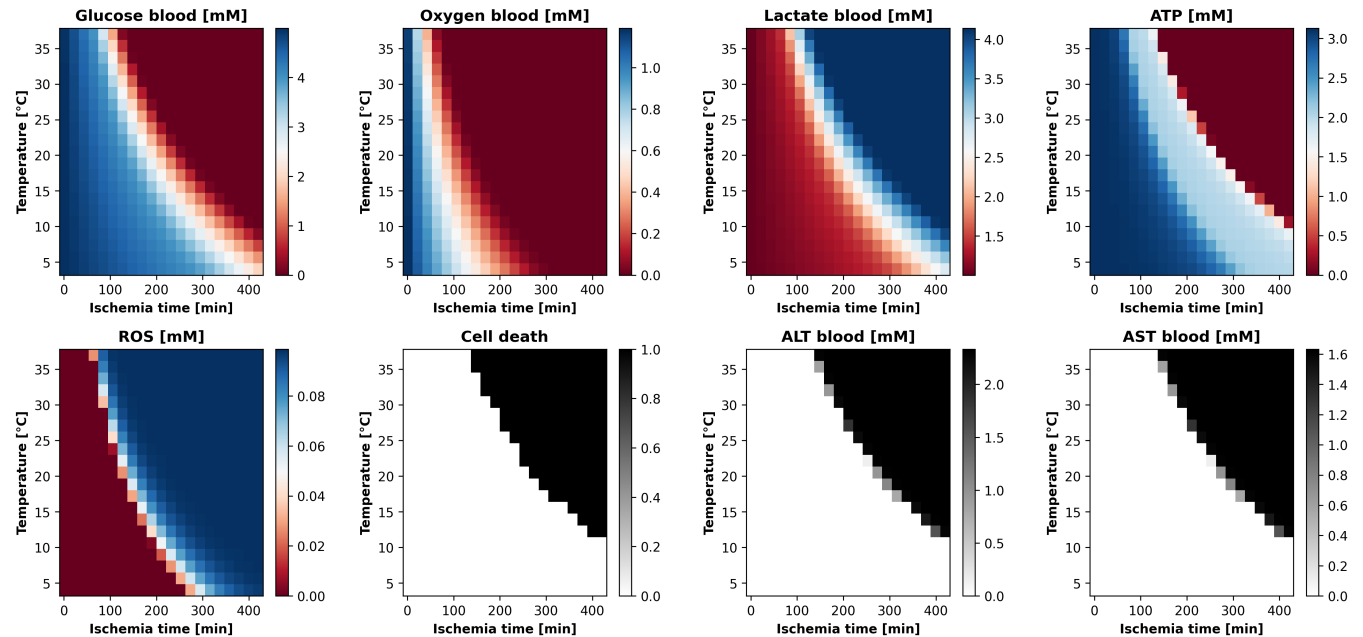


Figure 10 Variation of ischemia time and temperature (ODE perfusion model). Temperature was varied between 1°C 42°C and ischemia time between 1 min and 420 min. After an initial steady state under the given perfusion conditions at 37°C is reached, perfusion is stopped for the given ischemia time resulting in ischemia at the given temperature. The cellular state is depicted at the end of the ischemia period. Simulations corresponding to warm and cold ischemia at 37°C and 4°C for 180 min are indicated, corresponding to figure 8 and 9.

4.3 | PDE-ODE model of IRI

In a next step the cellular model of IRI was integrated into a multi-scale PDE-ODE model using a homogenized, multi-scale, multi-component approach within the TPM framework. For the coupling the SBML solver libroadrunner [36, 38] was integrated with the FEM software FEBio [22]. The cellular model is solved at every FEM point to provide the source and sink terms of the metabolites glucose, lactate, and oxygen in the fluid phase.

First, we tested the integration on a single volume element without perfusion or applied pressure and could confirm that in this case the coupled model behaves identically to the pure cell model at different temperatures (cf. figure 11). This is consistent with the expectations.

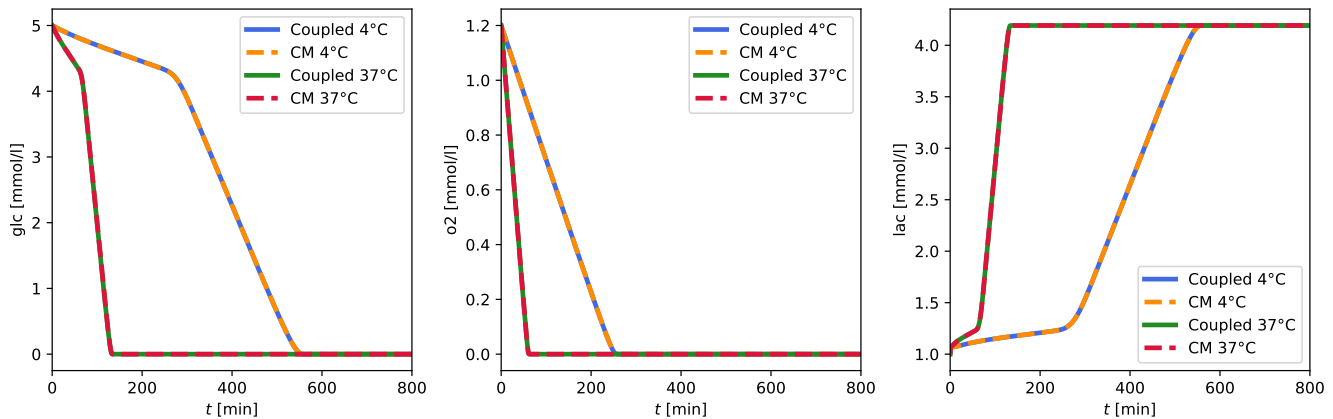


Figure 11 Comparison of the coupled model including lobular TPM/PDE model and the cellular ODE model with against solely the cellular model (CM) at two temperatures, i.e., 4°C and 37°C, without perfusion in the coupled model. Depicted are the three solutes glucose (glc), oxygen (o₂), and lactate (lac) over time t .

In a next step we simulated ischemia in a realistic lobulus geometry under different temperatures, i.e., warm ischemia conditions (at 37°C or 310.15 K) depicted in figure 12 and cold ischemia conditions (at 4°C or 277.15 K) depicted in figure 13. As boundary conditions we applied a prescribed pressure boundary of **Lena: Luis bitte ergänzen** at the portal triads and a prescribed pressure boundary of **Lena: @Luis: bitte ergänzen** at the central vein.

During the warm ischemia process (as shown in figure 12), there is a rapid depletion of oxygen within the initial hour. Concurrently, glucose levels start to diminish over a span of 180 minutes. This decrease in oxygen corresponds to an increase in lactate levels. As long as there is a sufficient supply of oxygen, ATP levels remain stable. However, they begin to drop around the 120-minute mark, which is the onset of anaerobic glycolysis. Upon complete utilization of the available glucose, hepatocytes lose their capacity to sustain ATP levels. This insufficiency triggers a necrotic process, which subsequently results in the release of ALT and AST. Furthermore, ischemia leads to an accumulation of reactive oxygen species. Because of the homogeneity of the initial conditions and the lack of perfusion, all hepatocytes exhibit the same behavior, creating a symmetrical response in the coupled problem.

In contrast, during cold ischemia (as detailed in figure 13), metabolic processes undergo a significant slowdown, leading to a reduced rate of oxygen and glucose consumption. This deceleration enables the liver tissue to withstand ischemic conditions for a considerably longer duration. As a result, ATP levels manage to stay high, and the formation of reactive oxygen species is not observed within the first three hours of cold ischemia. Necrosis is only apparent after approximately 600 minutes. Therefore, under cold conditions, liver tissue can stave off damage for an extended period.

4.4 | Conclusion

In this paper, we have presented a comprehensive review of the SimLivA project, along with our preliminary findings: a cellular model that delineates critical processes in the context of IRI during transplantation; and the integration of this model into a multi-scale PDE-ODE model using a homogenized, multi-scale, multi-component approach within the TPM framework. The

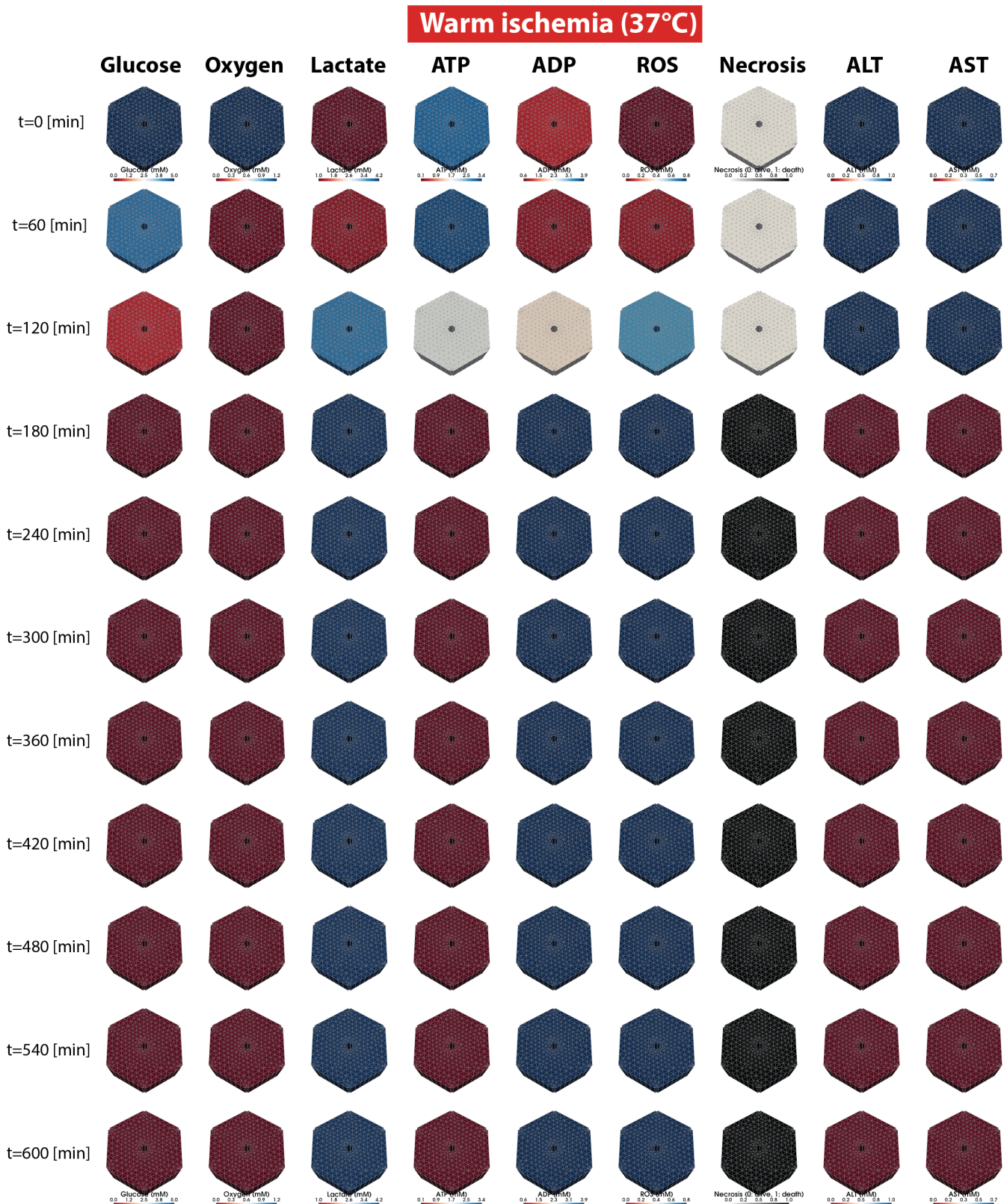


Figure 12 Warm ischemia at 37°C with the coupled PDE-ODE model in a realistic lobulus geometry. Ischemia (no perfusion) was simulated for 600 min.

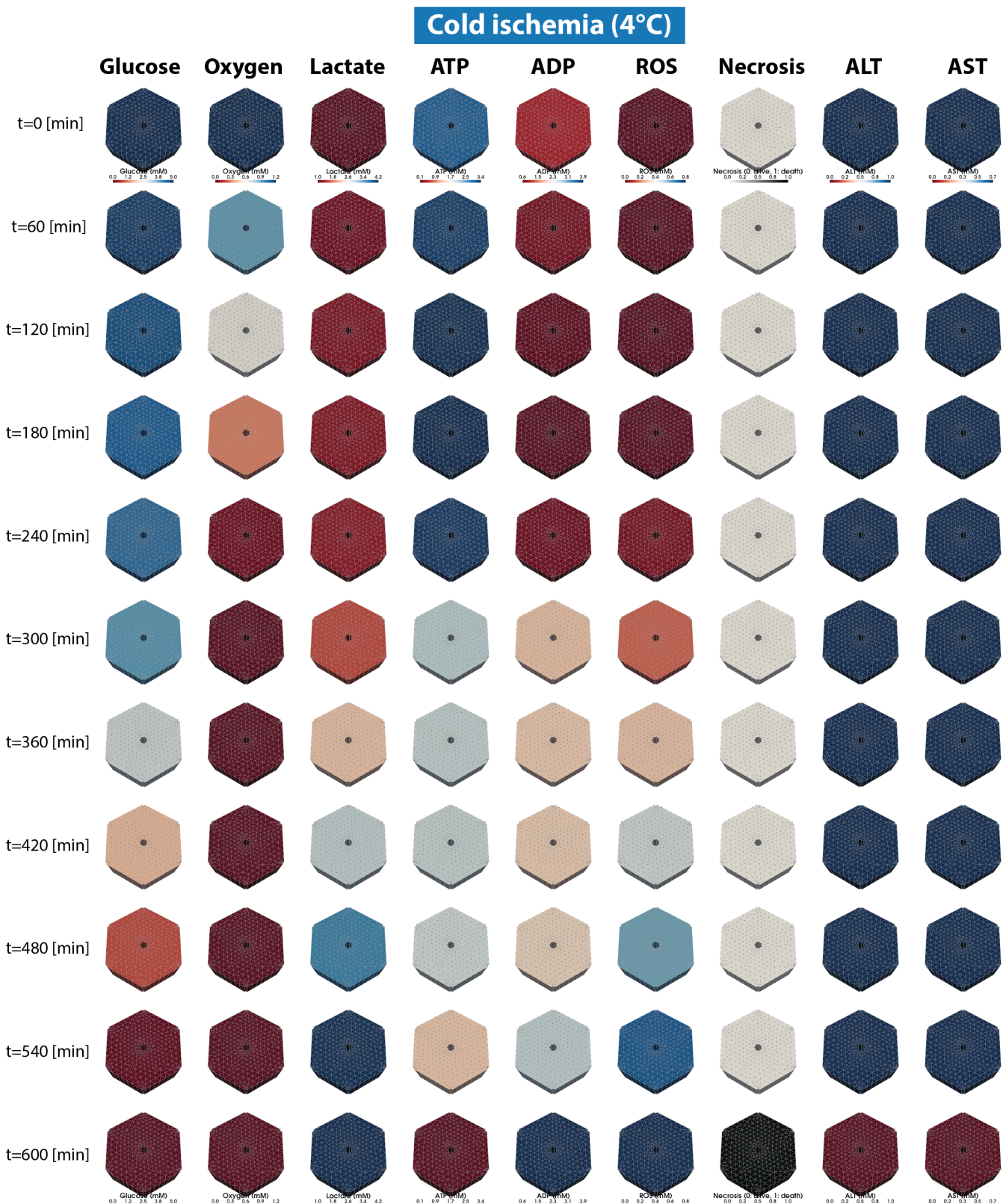


Figure 13 Cold ischemia at 4°C with the coupled PDE-ODE model in a realistic lobulus geometry. Ischemia (no perfusion) was simulated for 600 min.

model has successfully simulated the interconnected relationship between structure, perfusion, and function—all of which are integral to IRI. Additionally, we have been able to systematically study the impact of tissue perfusion and temperature, two critical parameters in the context of liver transplantation.

5 | OUTLOOK

In this study, we have laid the groundwork for enhancing and customizing a coupled continuum-biomechanical, multiphase, and multi-scale PDE-ODE model of the liver lobule. This advancement enables us to conduct numerical simulations of critical alterations in IRI, contingent upon the duration of ischemia and temperature.

In the future, we will augment our model simulations by incorporating heterogeneity into the coupled PDE-ODE problem. Specifically, we aim to include the element of inhomogeneous perfusion, as well as variability in cellular behavior depending on the position within the geometric framework - a phenomenon commonly referred to as hepatic zonation.

Integrating these factors will bring about a more comprehensive model that better mirrors the complex biological realities. The result of this will introduce spatial heterogeneity into our findings. This means the results will no longer be uniform across different spatial zones. Instead, they will reflect the rich and diverse behaviors that real biological systems exhibit across varied spatial dimensions and positions within a given geometry.

Currently, the temperature dependency is restricted to modifications of reaction rates in the metabolic ODE part of our model. A crucial forthcoming step will be the inclusion of temperature dependence on the PDE scale. Essential components such as material properties are temperature-dependent, as are transport processes like diffusion. Incorporating these factors will yield significant insights into how temperature variations influence the intricate relationships among material, perfusion, and liver function.

A second extension will be the coupling of an approach for fat accumulation in the cellular model and the tissue PDE model. Fat accumulation is a critical risk factor for the quality of the liver transplant. A major effect on the tissue scale is a change in perfusion/microcirculation, see [4, 20], which could further worsen the effects of ischemia, due to initial undersupply of the tissue. Also important material properties such as the stiffness of the liver will be parameterized using experimental and clinical data. The IRI model will be coupled to a fat metabolism on cellular scale, which result in a dynamical change of the fluid, solid and fat phases over time depending on the local cellular fat composition. The extended model will allow to study the additional effects of steatosis on the quality of the transplant and possible risks after liver transplantation.

Our envisioned model will intricately weave together the structure, perfusion, and function of the liver, thereby serving as a critical tool in clinical decision-making processes.

At present, the only clinically relevant method to effectively mitigate IRI is ex-vivo machine perfusion prior to implantation. Various strategies and devices are presently in operation, with variations in perfusion temperature (normothermic, hypothermic, subnormothermic), flow conditions (static, pulsatile, flow), and oxygenation (oxygenated, non-oxygenated, dual oxygenated) [6]. There is an urgent need for evidence supporting the optimal conditions for machine perfusion to alleviate IRI. Our long-term objective is to apply the developed model to fine-tune and individualize machine perfusion strategies.

ACKNOWLEDGMENTS

We thank the libroadrunner and SBML community for their support.

Author contributions

MK, TR, UD, and HMT conceptualized the project and secured the funding. MK developed the cellular ODE model for IRI in SBML and performed the respective analysis. TR, LM, LL, and SG developed the TPM model. MK, TR, LM, SG and LL developed the coupled PDE-ODE model and performed the respective analysis. UD and HMT conceptualized the experimental and clinical study. EL annotated the data for image analysis. All authors actively participated in the discussions of the results, contributed to critical revisions of the manuscript, and approved the final version for submission.

Financial disclosure

MK, TR, HMT, and LM were supported by grant number 465194077 (Priority Programme SPP 2311, Subproject SimLivA). MK, HMT, and TR were supported by the Federal Ministry of Education and Research (BMBF, Germany) within ATLAS by grant number 031L0304A, 031L0304B and 031L0304C. MK, TR, UD, and SG were supported within the Research Unit Program FOR 5151 "QuaLiPerF (Quantifying Liver Perfusion-Function Relationship in Complex Resection - A Systems Medicine Approach)" by grant number 436883643. LL and TR were supported by Deutsche Forschungsgemeinschaft (DFG, German Research Foundation) under Germany's Excellence Strategy – EXC 2075 – 390740016. LL is supported by the Add-on Fellowship of the Joachim Herz Foundation. This work was supported by the BMBF-funded de.NBI Cloud within the German Network for Bioinformatics Infrastructure (de.NBI) (031A537B, 031A533A, 031A538A, 031A533B, 031A535A, 031A537C, 031A534A, 031A532B).

Conflict of interest

The authors declare no potential conflict of interests.

References

- [1] W. B. Ashworth, N. A. Davies, and I. D. L. Bogle, *A computational model of hepatic energy metabolism: Understanding zonated damage and steatosis in nafld*, PLoS Computational Biology **12** (2016), no. 9, e1005105.
- [2] N. Berndt et al., *Hepatokin1 is a biochemistry-based model of liver metabolism for applications in medicine and pharmacology*, Nature communications **9** (2018), no. 1, 2386.
- [3] N. Boissier, D. Drasdo, and I. E. Vignon-Clementel, *Simulation of a detoxifying organ function: focus on hemodynamics modeling and convection-reaction numerical simulation in microcirculatory networks*, International journal for numerical methods in biomedical engineering (2020), e3422.
- [4] B. Christ et al., *Hepatectomy-induced alterations in hepatic perfusion and function - toward multi-scale computational modeling for a better prediction of post-hepatectomy liver function*, Frontiers in Physiology **12** (2021), 733868.
- [5] W. A. Dar et al., *Ischaemia reperfusion injury in liver transplantation: Cellular and molecular mechanisms*, Liver international : official journal of the International Association for the Study of the Liver **39** (2019), no. 5, 788–801.
- [6] V. E. de Meijer, M. Fujiyoshi, and R. J. Porte, *Ex situ machine perfusion strategies in liver transplantation*, Journal of hepatology **70** (2019), no. 1, 203–205.
- [7] C. Debbaut et al., *A 3d porous media liver lobule model: the importance of vascular septa and anisotropic permeability for homogeneous perfusion*, Computer methods in biomechanics and biomedical engineering **17** (2014), no. 12, 1295–1310.
- [8] K. He et al., *Mask R-CNN*, CoRR **abs/1703.06870** (2017). URL <http://arxiv.org/abs/1703.06870>.
- [9] M. Hucka et al., *The Systems Biology Markup Language (SBML): Language specification for Level 3 Version 2 Core Release 2*, Journal of integrative bioinformatics **16** (2019), no. 2.
- [10] K. Jungermann and T. Kietzmann, *Zonation of parenchymal and nonparenchymal metabolism in liver*, Annual review of nutrition **16** (1996), 179–203.
- [11] S. M. Keating et al., *SBML Level 3: an extensible format for the exchange and reuse of biological models*, Molecular systems biology **16** (2020), no. 8, e9110.
- [12] M. König, *sbmlsim: SBML simulation made easy* (2021). URL <https://doi.org/10.5281/zenodo.5531088>.
- [13] M. König, *sbmlutils: Python utilities for SBML* (2023). URL <https://doi.org/10.5281/zenodo.8115269>.
- [14] M. König, A. Dräger, and H.-G. Holzhütter, *CySBML: A Cytoscape plugin for SBML*, Bioinformatics **28** (2012), no. 18, 2402–2403.

- [15] M. König and N. Rodriguez, *matthiaskoenig/cy3sbml: Cy3sbml-v0.3.0 - SBML for Cytoscape*, 2019, . URL <https://doi.org/10.5281/zenodo.3451319>.
- [16] T. Köppl, E. Vidotto, and B. Wohlmuth, *A 3d-1d coupled blood flow and oxygen transport model to generate microvascular networks*, International journal for numerical methods in biomedical engineering **36** (2020), no. 10, e3386.
- [17] M. König, *Hepatocyte model of ischemia reperfusion injury (IRI)* (2023). URL <https://doi.org/10.5281/zenodo.8100329>.
- [18] M. König, S. Bulik, and H.-G. Holzhütter, *Quantifying the contribution of the liver to glucose homeostasis: a detailed kinetic model of human hepatic glucose metabolism*, PLoS computational biology **8** (2012), e1002577.
- [19] M. König and H.-G. Holzhütter, *Kinetic modeling of human hepatic glucose metabolism in type 2 diabetes mellitus predicts higher risk of hypoglycemic events in rigorous insulin therapy.*, The Journal of biological chemistry **287** (2012), 36978–36989.
- [20] L. Lambers, *Multiscale and multiphase modeling and numerical simulation of function-perfusion processes in the liver*, 2023, . URL <http://elib.uni-stuttgart.de/handle/11682/13061>.
- [21] L. Lambers, T. Ricken, and M. König, *A multiscale and multiphase model for the description of function-perfusion processes in the human liver*, A. Zingoni, (ed.), *Advances in Engineering Materials, Structures and Systems: Innovations, Mechanics and Applications*, CRC Press, 2019. 304–307, .
- [22] S. A. Maas et al., *FEBio: Finite elements for biomechanics*, Journal of Biomechanical Engineering **134** (2012), no. 1. URL <https://doi.org/10.1115/1.4005694>.
- [23] S. Mitchell and P. Mendes, *A computational model of liver iron metabolism*, PLoS computational biology **9** (2013), no. 11, e1003299.
- [24] S. Moosburner et al., *Nicht transplantierte Spenderorgane – eine bundesweite Auswertung aller Organangebote für die Lebertransplantation von 2010 bis 2018*, Zeitschrift fur Gastroenterologie **58** (2020), no. 10, 945–954.
- [25] J. Palanichamy et al., *Simulation of ammonium and chromium transport in porous media using coupling scheme of a numerical algorithm and a stochastic algorithm.*, Water science and technology : a journal of the International Association on Water Pollution Research **59** (2009), 1577–1584.
- [26] E. N. G. d. S. Pereira et al., *Hepatic microvascular dysfunction and increased advanced glycation end products are components of non-alcoholic fatty liver disease*, PloS one **12** (2017), no. 6, e0179654.
- [27] H. P. Rani et al., *Numerical investigation of non-newtonian microcirculatory blood flow in hepatic lobule*, Journal of biomechanics **39** (2006), no. 3, 551–563.
- [28] D. Reddyhoff et al., *Timescale analysis of a mathematical model of acetaminophen metabolism and toxicity*, Journal of theoretical biology **386** (2015), 132–146.
- [29] T. Ricken, U. Dahmen, and O. Dirsch, *A biphasic model for sinusoidal liver perfusion remodeling after outflow obstruction*, Biomechanics and modeling in mechanobiology **9** (2010), no. 4, 435–450.
- [30] T. Ricken and L. Lambers, *On computational approaches of liver lobule function and perfusion simulation*, GAMM-Mitteilungen **42** (2019), no. 4, e201900016.
- [31] T. Ricken, N. Waschinsky, and D. Werner, *Simulation of Steatosis Zonation in Liver Lobule—A Continuummechanical Bi-Scale, Tri-Phasic, Multi-Component Approach*, Peter Wriggers, Prof. Thomas Lenarz, (ed.), *Biomedical Technology*, vol. 84, Springer International Publishing, 2018. 15–33, .
- [32] T. Ricken et al., *Modeling function-perfusion behavior in liver lobules including tissue, blood, glucose, lactate and glycogen by use of a coupled two-scale pde-ode approach*, Biomechanics and modeling in mechanobiology **14** (2015), no. 3, 515–536.

- [33] J. Schleicher et al., *A theoretical study of lipid accumulation in the liver-implications for nonalcoholic fatty liver disease*, *Biochimica et biophysica acta* **1841** (2014), no. 1, 62–69.
- [34] L. O. Schwen et al., *Zonated quantification of steatosis in an entire mouse liver*, *Computers in biology and medicine* **73** (2016), 108–118.
- [35] L. P. Smith et al., *SBML Level 3 package: Hierarchical model composition, Version 1 Release 3*, *Journal of integrative bioinformatics* **12** (2015), no. 2, 268.
- [36] E. T. Somogyi et al., *libroadrunner: a high performance sbml simulation and analysis library*, *Bioinformatics* (Oxford, England) **31** (2015), no. 20, 3315–3321.
- [37] K. van Eunen et al., *Biochemical competition makes fatty-acid β -oxidation vulnerable to substrate overload*, *PLoS computational biology* **9** (2013), no. 8, e1003186.
- [38] C. Welsh et al., *libRoadRunner 2.0: A high performance SBML simulation and analysis library*, *Bioinformatics* **39** (2023), no. 1, btac770.
- [39] D. Werner et al., *On the influence of growth in perfusion dependent biological systems - at the example of the human liver*, *PAMM* **15** (2015), no. 1, 119–120.

